Knowl Inf Syst (2010) 24:91–111
DOI 10.1007/s10115-009-0225-z

REGULAR PAPER

# Fuzzy entropy based optimization of clusters for the segmentation of lungs in CT scanned images

**M. Arfan Jaffar · Ayyaz Hussain · Anwar Majid Mirza**

Received: 30 December 2008 / Revised: 4 May 2009 / Accepted: 17 May 2009 /
Published online: 25 June 2009


**Abstract** In this paper, we have proposed a method for segmentation of lungs from Computed Tomography (CT)-scanned images using spatial Fuzzy C-Mean and morphological techniques known as Fuzzy Entropy and Morphology based Segmentation. To determine dynamic and adaptive optimal threshold, we have incorporated Fuzzy Entropy. We have proposed a novel histogram-based background removal operator. The proposed system is capable to perform fully automatic segmentation of CT Scan Lung images, based solely on information contained by the image itself. We have used different cluster validity functions to find out optimal number of clusters. The proposed system can be used as a basic building block for Computer-Aided Diagnosis. The technique was tested against the 25 datasets of different patients received from Aga Khan Medical University, Pakistan. The results confirm the validity of technique as well as enhanced performance.

**Keywords** Computer aided diagnosis · Mathematical morphology · Segmentation · Thresholding

## 1 Introduction

Image segmentation refers to the process of partitioning a digital image into multiple regions (sets of pixels). Each of the pixels in a region is similar with respect to some characteristic or computed property, such as color, intensity, or texture. Adjacent regions are significantly

M. A. Jaffar (✉) · A. Hussain · A. M. Mirza
Department of Computer Science,
FAST National University of Computer and Emerging Sciences,
A.K. Brohi Road, H-11/4, Islamabad, Pakistan
e-mail: arfan.jaffar@nu.edu.pk

A. Hussain
e-mail: ayyaz.hussain@nu.edu.pk

A. M. Mirza
e-mail: anwar.m.mirza@nu.edu.pk

different with respect to the same characteristic(s) [2]. High-resolution X-Ray computed tomography (CT) is the standard for pulmonary imaging. CT scan can give high-spatial and temporal resolutions based on the hardware used for scanning. It can also give outstanding contrast resolution for the pulmonary structure. It has the ability to get together a complete three-dimensional (3-D) volume of the human thorax in a single breath clutch. For diagnosing early lung cancer, pulmonary CT-scanned images have been used for applications such as lung parenchyma airways analysis, density analysis [7], and nodule detection. Lung segmentation is a precursor to all of these quantitative analysis applications.

Computer Aided Diagnosis (CAD) of lung CT image has been an important and innovative development, in the early and untimely detection of lung abnormalities. The CAD systems comprise of systems needed for 'automatic detection of abnormality nodules' and '3-D reconstruction of lung'. Combined together, these systems support the radiologists in their final decisions. Image processing algorithms and techniques are applied on the images to elucidate and enhance the image. Later, these are applied to separate the area of interest from the whole image. Radiologists study and analyze these separately obtained areas, which are then used for the detection of nodules in order to diagnose the disease [15]. The accuracy and higher decision confidence value of any lung abnormality identification system relies profoundly on an efficient lung segmentation technique. It is, therefore, very important for effective performance of these systems to provide them with entire and perfectly complete lung part of the image. No part of interest that is part of the original image be eradicated.

However, there are several issues related to image segmentation that require a detailed review. One of the common problems encountered in image segmentation is choosing of a suitable approach for isolating different objects from the background. For example in case of Lung CT Scan, segmentation can be performed by making use of excellent contrast between air and surrounding tissues. However, this approach fails when lung is affected by high-density pathology. Moreover, for computer analysis such as detection and quantification of abnormal areas, it is vital that the entire and perfectly complete lung part of the image is provided and no part, as present in the original image, be eradicated [1]. An additional problem is the inaccurate lung segmentation due to the juxtapleural nodules present at the border of chest wall in lung parenchyma.

Main contributions of the Fuzzy Entropy and Morphology based Segmentation (FEMS) technique include

- It is completely automatic and unsupervised method.
- No prior assumption is made about the image (features, type, contents, stochastic model, etc.).
- FEMS technique has a novel background removal operator based on histogram of the image that removes the background very intelligently and fully automatically.
- It is robust against noise due to incorporation of spatial Fuzzy c-means (FCM).
- Segments have been validated by using different cluster validity functions.
- FEMS technique finds out optimal and dynamic threshold by using fuzzy entropy.
- Edge detection is performed by using morphology image processing technique that helps to remove noise.

This FEMS method ensures that no nodule information is lost after segmentation. This will help us for better classification of nodules.

The rest of the paper is organized as follows. Section 2 contains a survey on prior research that is most closely related to the present work. In particular, fuzzy C-Mean method, some cluster validity measures and fuzzy based entropy measures are reviewed. A detailed description of the FEMS system follows (Sect. 3). Data characteristics are presented

in (Sect. 4). Implementation and relevant results are presented in Sect. 5. Finally, Sect. 6 ends the paper with several conclusions drawn from the design and the working of the FEMS system.

## 2 Related work

Antonelli et al. [14] have used background-removal operator and iterative gray level thresholding methodology for lung segmentation. Background cannot be eliminated completely when there is noise at the corners. It also fails when the lung portion is connected to the boundary of the image. However, the presence of a distinct outer black region is a prerequisite for their accurate and precise performance. This region should enclose the whole lung parenchyma and the adjoining features. Gwadera et al. [18] have developed an Optimal segmentation using tree models. Cesario et al. [6] have proposed a Boosting text segmentation via progressive classification. Haiminen et al. [17] have proposed an algorithms for unimodal segmentation with applications to unimodality detection.

Samuel et al. [20] have used Ball-Algorithm for the segmentation of lungs. Gray level thresholding process has been used and applied at each CT image. The major purpose of this process is to segment the thorax from background and then the lungs from the thorax area. After then, rolling ball algorithm is used for lung segmentation contours, acquired in the first stage. The major advantage of application of this algorithm is to avoid the loss of juxtapleural nodules. The main drawback of this technique is the size of the ball selected for morphological operation. It has been observed that selected ball size for morphological closing did not work for the whole database of a single patient. Sometimes, a ball of specified size worked for one patient while it was not enough for another patient. Thus, we have to vary the ball size patient-by-patient which makes the algorithm semi-automatic.

Binsheng et al. [5] have used histogram for threshold selection. Then this threshold is used to separate the lung parenchyma from the other anatomical structures on the CT images in the first stage. There is always a difference in the apparent density of voxels and bronchial walls in the lungs of CT-scanned images. Thus, it can be possible that structures with higher densities including some higher density nodules could be grouped into soft tissues and bones. As a result, it produces an incomplete extraction of lung mask. In order to obtain complete hollow-free lung mask, morphological closing is applied. Morphological operators help to choose spherical shape of the structural element so that filter size can be approximately determined. With the help of 3-D mask, the lungs can be readily extracted from the original chest CT images [16].

An automatic CAD system for lung-cancer screening was developed by El-Baz et al. [3]. For this purpose, they have used chest spiral CT scans. This paper presents the first phase of an image analysis system for 3-D reconstruction of the lungs and trachea, detection of the lung abnormalities, identification or classification of these abnormalities with respect to specific diagnosis. Optimal gray-level thresholding is applied by El-Baz et al. [4] for the extraction of thorax area. After the selection and application of threshold, region growing and connectivity analysis are used for extraction of the exact cavity region with predetermined accuracy. Some outstanding results have been observed using this scheme for all CT-sections having distinctive intensities of lung parenchyma. But these techniques do not perform well when there is overlapping of intensities in lung parenchyma and surrounding chest wall [24].

Shiying et al. [21] have developed an automatic method for identifying lungs in 3-D pulmonary X-Ray CT images. They have divided their work into three main stages: (1) Gray-level thresholding has been used to extract lung from CT-Scan image (2) left and right

lungs are separated through identification of the anterior and posterior junctions by using dynamic programming and (3) to smooth the irregular boundary along the mediastinum, a sequence of morphological operations for acquiring results. It can be observed that this technique has the following very serious shortcomings: (i) Fixed ball size (ii) addition of unnecessary areas as lung regions (iii) Processing time overhead. It can also be observed that the ball algorithm includes the unnecessary areas as the lung region, (not actually the part of the lung) [16].

Thus if such a situation arises, these approaches are most likely to yield poor results. Thus, we can say that these methodologies only work partially.

In [11] a shape-based genetic algorithm template-matching method has been proposed for the detection of nodules with spherical elements. In [13] the key step is identification of structures in several applications of medical imaging. They have proposed a method for the identification of structures using a multiscale approach with inclusion of a priori information about the searched objects. Thus due to inclusion of a prior information, it is not fully automatic. But our method is completely and fully automatic. There is no need of prior information about the images in our proposed method.

### 2.1 Spatial FCM clustering

Fuzzy c-means is a method of clustering which allows one piece of data to be in the right position to two or more clusters. This method (developed by Dunn in 1973 and improved by Bezdek [10]) is frequently used in pattern recognition. FCM starts with an initial guess for the cluster centers, which are FEMS to mark the mean location of each cluster. The initial guess for these cluster centers is most likely incorrect. Additionally, FCM assigns every data point a membership rank for every cluster. By iteratively updating the cluster centers and the membership grades for each data point, FCM iteratively moves the cluster centers to the correct place within a dataset. This iteration is based on minimizing an objective function that symbolizes the distance from any given data point to a cluster center weighted by that data point's membership rank [10].

One of the significant uniqueness of an image is that neighboring pixels are extremely correlated. In other terms, these neighboring pixels hold similar feature values, and the probability that they belong to the same cluster is great. This spatial relationship is important in clustering, but it is not utilized in a standard FCM algorithm. To develop the spatial information, a spatial function $h_{ij}$ is defined as

$$h_{ij} = \sum_{k \in NB(x_j)} U_{ik} \tag{1}$$

where NB $(x_j)$ stands for a square window centered on pixel $x_j$ in the spatial domain and $i$, $j$ are data points. A $3 \times 3$ window was used throughout this work. Just like the membership function, the spatial function $h_{ij}$ stands for the probability that pixel $xj$ belongs to $i$th cluster. The spatial function of a pixel for a cluster is large if the bulk of its neighborhood belongs to the same clusters. The spatial function is included into membership function $U'_{ij}$ as follows:

$$U'_{ij} = \frac{U_{ij}^{p} h_{ij}^{q}}{\sum_{k=1}^{C} U_{kj}^{p} h_{kj}^{q}} \tag{2}$$

where $p$ and $q$ are parameters to control the relative importance of both functions and $i$, $j$ are data points. In a homogenous region, the spatial function simply fortifies the original membership, and the clustering result remains unchanged. However, for a noisy pixel, this

formula reduces the weighting of a noisy cluster by the labels of its neighboring pixels. As a result, misclassified pixels from noisy regions or spurious blobs can easily be corrected. Note that spatial Fuzzy C-Mean 1,0 is identical to the conventional FCM. The clustering is a two-pass process applied at each iteration. The first pass is the same as that in standard FCM to calculate the membership function in the spectral domain. In the second pass, the membership information of each pixel is mapped to the spatial domain, and the spatial function is computed from that. The FCM iteration proceeds with the new membership that is incorporated with the spatial function. The iteration is stopped when the maximum difference between two cluster centers at two successive iterations is less than a threshold (0.02). After the convergence, defuzzification is applied to assign each pixel to a specific cluster for which the membership is maximal.

### 2.2 Cluster validity function

Two types of cluster validity functions, fuzzy partition and feature structure, are often used to evaluate the performance of clustering in different clustering methods [10]. The representative functions for the fuzzy partition are partition coefficient $V_{pc}$ and partition entropy $V_{pe}$. They are defined as follows:

$$V_{pe} = \frac{-\sum_j^N \sum_i^C U_{ij} \log U_{ij}}{N} \tag{3}$$

and

$$V_{pc} = \frac{-\sum_j^N \sum_i^C U_{ij}^2}{N} \tag{4}$$

where $N$ the total number of points and $C$ is the number of clusters and $i$, $j$ are data points. The idea of these validity functions is that the partition with less fuzziness means better performance. As a result, the best clustering is achieved when the value $V_{pc}$ is maximal or $V_{pe}$ is minimal. Disadvantages of $V_{pc}$ and $V_{pe}$ are that they measure only the fuzzy partition and lack a direct connection to the featuring property. Other validity functions based on the feature structure are available [10]. For example, Xie and Beni [23] defined the validity function as

$$V_{xb} = \frac{\sum_j^N \sum_i^C U_{ij}^2 \left\| X_j - V_i \right\|^2}{N * (\min i \neq k) \left\{ \| V_k - V_i \|^2 \right\}} \tag{5}$$

where $X$ is original data point and $V$ is the center of cluster. A good clustering result generates samples that are compacted within one cluster and samples that are separated between different clusters. Minimizing $V_{xb}$ is expected to lead to a good clustering. Xie and Beni validity function is considered to as a better validity function amongst others.

## 3 FEMS method

### 3.1 Overview of the FEMS system

The FEMS method is a combination of image processing techniques and fuzzy logic applied to each slice. More precisely, the following steps are performed:

- The background (i.e., the pixels outside the lungs) is removed from the image by using a new histogram-based technique.
- Cluster validity is performed by using spatial Fuzzy C Mean and different cluster validity measures.
- A fuzzy entropy-based threshold technique is used to produce a binary image.
- Edge detection based upon morphological operations are applied; in particular, the opening operator is adopted to eliminate the small objects inside the lung and to separate some regions that should be separate but are joined by a thin area of foreground pixels, whereas the closing operator aims to get rid of small holes that represent border interruptions.
- Cleaning is performed to remove small noise
- Thinning is used to reduce the border size to one pixel by using SUSAN thinning algorithm.
- Reconstruction of pulmonary lobe's border is performed by an operator which, based on the border shape, reinserts erroneously erased zones; in particular, the nodules adjacent to the pleura that have been eliminated by thresholding are recovered
- Filling operator is applied to the pulmonary lobes chains, thus reintroducing the correct values of grey levels inside the lungs.
- Lung part is separated from original image.

In the following, the various steps of the method are described with more details.

### 3.2 System description

The FEMS system is based on fuzzy logic and morphology image processing techniques that perform automatic, adaptive, and optimal thresholding of the image using labels automatically, pre-selected by a fuzzy clustering technique. Fuzzy entropy is used as a measure for determining the optimal threshold.

A general flowchart of the FEMS algorithm is depicted in Fig. 1. We have divided our technique into different blocks as shown in Fig. 2.

#### *3.2.1 Preprocessing (Background Removal)*

By simply applying a threshold to the image, one cannot eliminate whole background as there is high similarity between the gray levels of the lungs and the image background as shown in the Fig. 3a. Therefore, there is a need for a mechanism to remove the whole background. Different techniques have been developed to remove the background. The most promising technique that provides good results has been developed in [14]. First, the background is removed by using a background removal operator. This operator starts from the four corners of the image, moves along the four directions identifying those pixels with a gray level within a range as background pixels and removing the pixels. The technique which is described in [14] has some draw backs. When it is applied on some images the whole background is not removed as shown in the Fig. 3b. The background that is left is mostly on the center top and center bottom. This is due to the fact this boundary is sandwiched between the lungs portion and, therefore, cannot be eliminated using the technique in [14]. Another major drawback of this technique is that it fails to remove the boundary if the image is skewed or not in proper coordinates. If the image is slightly rotated so that corners of the lung image becomes outside the background range or due to noise corners also have been changed as shown in the Fig. 3c, then this technique will also fail to remove the background sufficiently as shown in Fig. 3d.

To overcome this problem we work with another approach in which along with starting from all four corner points, we started traversing the image from middle of the top and

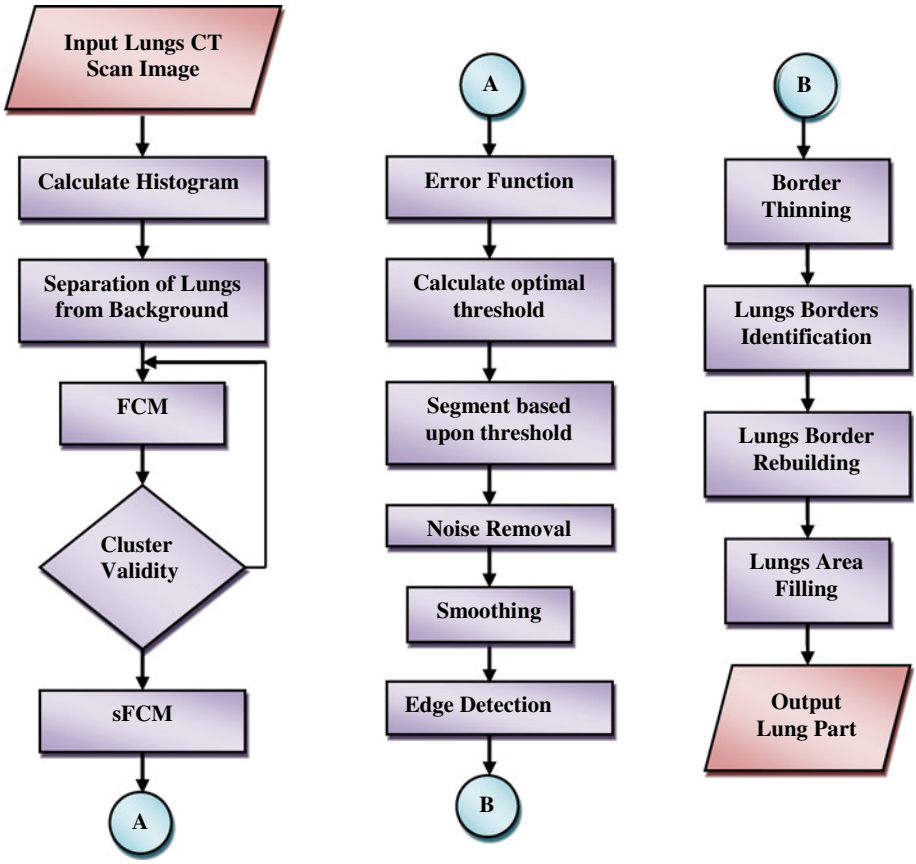


**Fig. 1** Flow chart of FEMS system

bottom. This was an extension to the work done in [14], but it did not completely resolve the problem. This technique works very well with images as shown in the figure, but it also did not resolve the problem of rotated images or in the case of noise in which corners of the image changed. Also it did not cater to the problem when the background was not exactly in the middle. So, we needed to work with an altogether different approach which we have developed and is described below. Thus, the major problem in the previous technique is the seed point. From where the operator has to start to remove background. So we have provided a novel technique to remove background fully automatically. This technique works as well. The technique starts traversing the image from start of the first column and traverses the whole boundary finishing at the same point where it started. While traversing, it keeps track of all the pixel values and plots them in the form of histogram. When applied experimentally, it showed regions of the background attached to the boundary. So the histogram properly showed peaks and valleys as shown in the Fig. 4.

Once this histogram is obtained, we can start at any point in the grey level region (background area) and start removing it until the background area is finished. This process provides us a seed point to start background removal operator. The advantage we have using this technique is that, with the help of histogram, we now exactly know where the background area lies in the image and we remove all those areas. This technique also worked

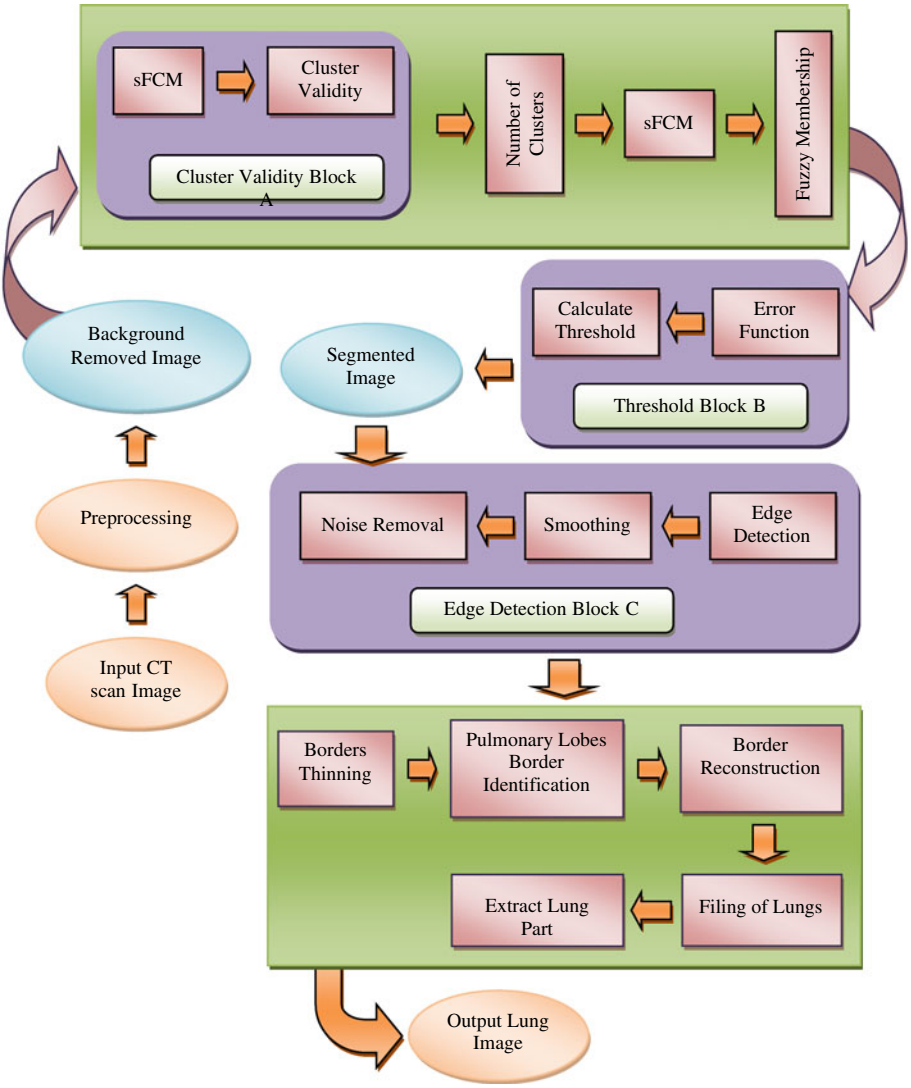


**Fig. 2** Block diagram of FEMS system

in the case of noise or for those images whose corners have changed. Thus, we achieve fully automated and complete background removal process as shown in Fig. 7b. The image resulting from the application of this operator consists of just the chest and the lungs, as shown in Fig. 5b.

### *3.2.2 Cluster validity block A*

After removing background as pre-processing, we find out histogram and the FCM algorithm was employed to create a fuzzy partition that properly describes the image, using only the pixel intensity feature. In order to keep the system totally autonomous, an automatic way

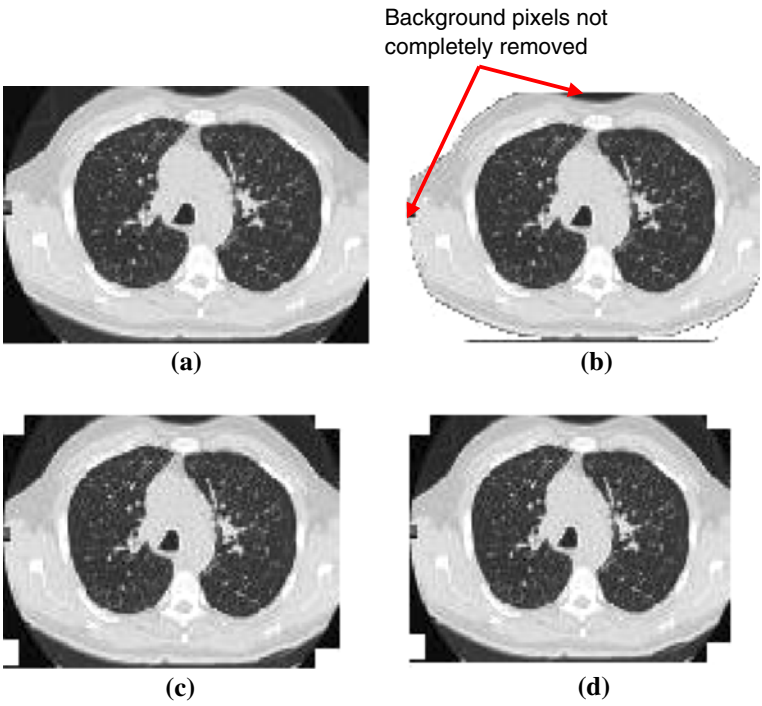


**Fig. 3** Background removal results [14] **a** Original image, **b** background removed image by using technique [14], **c** Original image degraded due to noise, **d** background removed image by using technique [14]

to determine the right number of clusters is needed. In the FEMS system, this was done by iterating the FCM algorithm for a range of hypothesized numbers of clusters and choosing the best option based on a cluster validity measure. Although in general, cluster validity measures are not considered very reliable. Some of them (e.g., the partition coefficient and the partition entropy, [12]) yielded surprisingly good results for some of the test images. These measures shows promising results on the medical images as shown in Table 1 and 2.

After finding out optimal number of clusters, we pass these optimal clusters to the spatial FCM. Spatial FCM also consider neighboring information of each pixel and return fuzzy membership matrix. Spatial information incorporated by FCM helps us to remove noise in the image as well.

### *3.2.3 Optimal threshold (Block B)*

There are variable numbers of slices in each CT scan. It is not necessary that all slices contain useful information for our purposes. Actually, the lungs appear only at the first and last slice of the CT scan images and these slices do not coincide with each other. Order number of slices varies from one examination to another of CT scan. There are two types of slices: one is called as useless slices and other is called as useful slices. There are few initial and final slices that might not contain any lung images and these slices can be called as useless slices and remaining slices are called as useful slices. We can still identify three different groups corresponding, respectively, to the upper, middle, and lower parts of the lung volume. Indeed, in the upper and lower parts, the lung region occupies a much smaller percentage of each

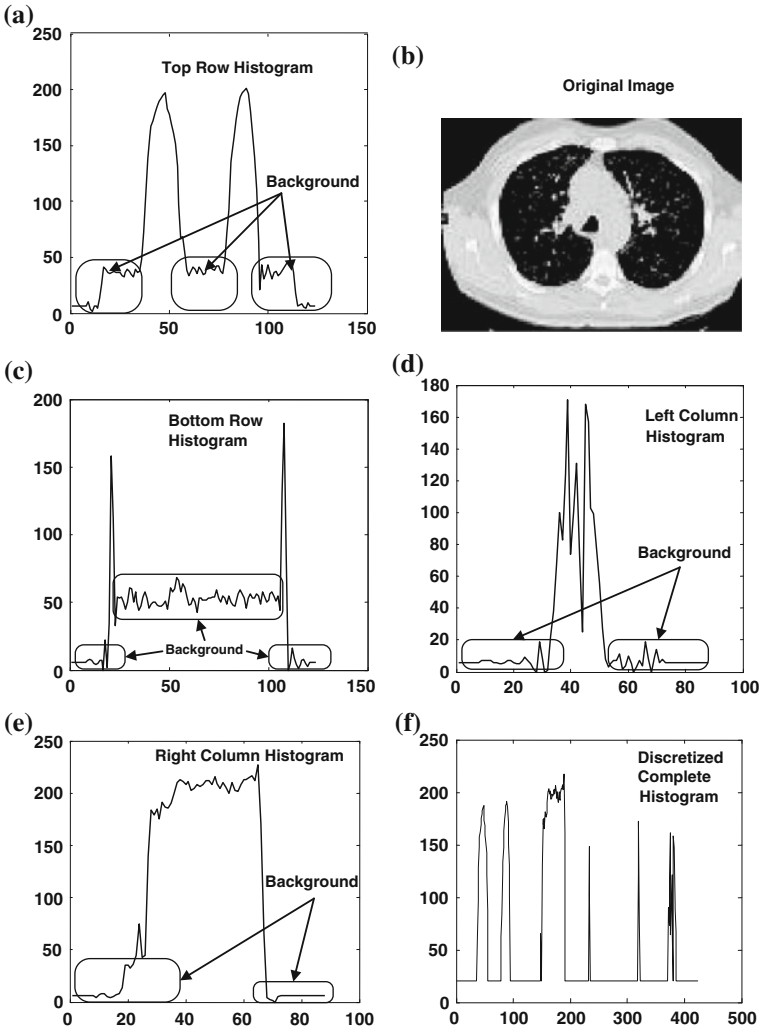


**Fig. 4** Histogram of top, bottom, left, and right-side boundaries

slice image than happens in the middle part. Consequently, we have to adopt different threshold techniques depending on the type of slice to be processed: we use an optimal, dynamic threshold for the slices of the lung middle part and a threshold determined empirically for all other slices.

There are different methods to compute optimal threshold. We have implemented a lot of those methods and found out a lot of problems. We have found that all those methods work well only with respect to some images but fail when applied to some different types of images or in case of noisy images. Most methods fail to provide good results. All previous methods have to choose an initial threshold that is also a very big problem. Most methods use mean as an initial threshold but it fails in case of noisy images because mean is not robust for noise. So, we have used a method based upon fuzzy entropy that finds out optimal and dynamic thresholds according to the clusters found out by using the well-known method of FCM.

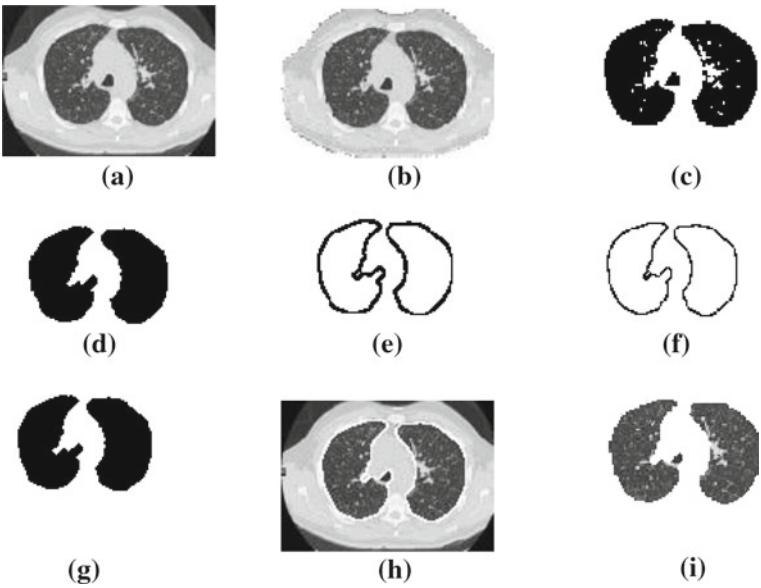


**Fig. 5** Results of FEMS system algorithms step by step. **a** Original, **b** Background removal, **c** Threshold, **d** After morphology, **e** Lung border recognition, **f** Lung border thinning, **g** Lung area filling, **h** Restored, **i** Segmented

**Table 1** Index values from 2 to 10 clusters in three different schemes. Shaded blocks show the correct results for image1

| Index | C=2 | C=3 | C=4 | C=5 | C=6 | C=7 | C=8 | C=9 | C=10 |
|---|---|---|---|---|---|---|---|---|---|
| PC | 0.57 | **0.72** | 0.58 | 0.56 | 0.53 | 0.51 | 0.50 | 0.44 | 0.40 |
| PE | 0.08 | **0.03** | 0.13 | 0.18 | 0.32 | 0.36 | 0.48 | 0.44 | 0.56 |
| XB | 0.21 | **0.12** | 0.26 | 0.32 | 0.32 | 0.34 | 0.38 | 0.39 | 0.49 |

**Table 2** Index values from 2 to 10 clusters in seven different schemes. Shaded blocks show the correct results for image2

| Index | C=2 | C=3 | C=4 | C=5 | C=6 | C=7 | C=8 | C=9 | C=10 |
|---|---|---|---|---|---|---|---|---|---|
| PC | 0.66 | **0.82** | 0.68 | 0.62 | 0.61 | 0.54 | 0.52 | 0.40 | 0.37 |
| PE | 0.21 | **0.10** | 0.18 | 0.26 | 0.37 | 0.35 | 0.38 | 0.47 | 0.52 |
| XB | 0.11 | **0.09** | 0.25 | 0.31 | 0.32 | 0.38 | 0.39 | 0.42 | 0.43 |

This method works as follows: First, it finds out histogram of the image after background removal. Then applies FCM to partition the image into different constituent parts and tries to find out clusters. We have also tried to validate those clusters by using some well-known cluster validity measures. We have taken this step so that we can analyze how many types of groups in our image.

This stage provides an objective error function that is used to find out adaptive, optimal, and dynamic threshold which is used in the next stage to segment the image. Output image of the background removal stage is used as input in this stage. First, this image is used to find histogram. Then based upon gray level histogram, it is fuzzified and then the error function is obtained by determining the contribution of each gray level to the fuzzy entropy of the partition (any fuzziness measure can be employed).

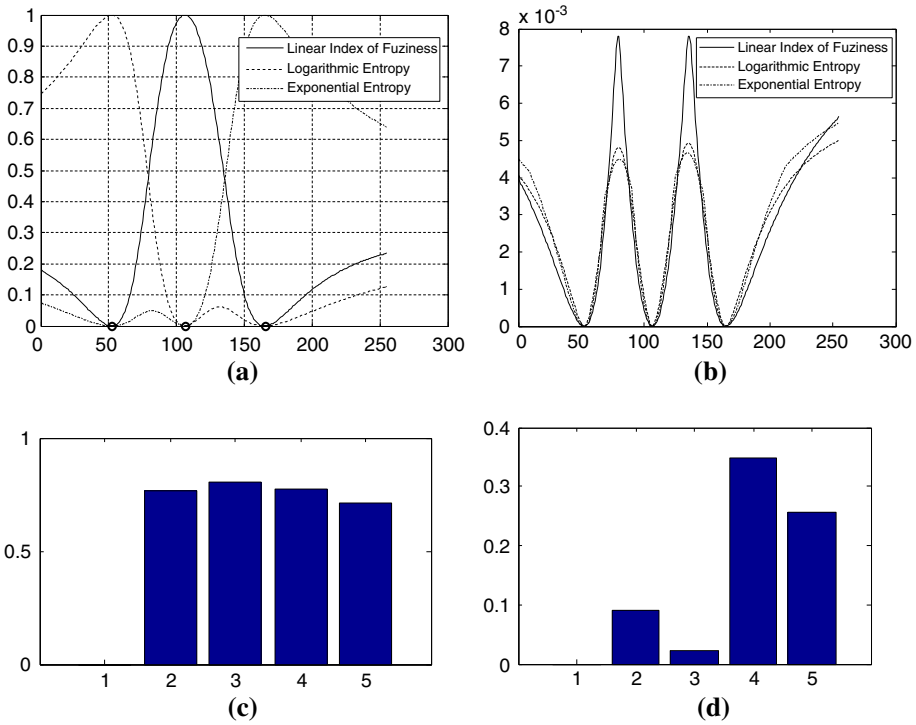


**Fig. 6** Preprocessing and fuzzy entropy. **a** Fuzzy membership, **b** Fuzzy entropies by Eq. (3, 4, 5), **c** Cluster validity of Eq. (7), **d** Cluster validity of Eq. (6)

We have used three different fuzzy entropy-based error functions aS depicted in Fig. 6a and b. The threshold values are obtained from the error function, as the gray levels with the maximal levels of fuzziness, respectively [22].

Linear Index of Fuzziness

$$v_l\,(\mathrm{A}) = \frac{2}{n}\sum_{i=1}^{n}\left|\mu_A\,(x_i) - \mu_{\underline{A}}\,(x_i)\right| v_l\,(\mathrm{A}) = \frac{2}{n}\sum_{i=1}^{n}\left[\min\left\{\mu_A\,(x_i)\,(1-\mu_A\,(x_i))\right\}\right] \quad (6)$$

Logarithmic Entropy

$$\mathrm{H(A)} = -\frac{1}{n\ln(2)}\sum_{i}\left[\mu_A\,(x_i \ln \mu_A(x_i + (1-\mu_A\,(x_i)) * (1-\ln \mu_A(x_i)))\right] \quad (7)$$

Exponential Entropy

$$\mathrm{H\,(A)} = \frac{1}{n\left(\sqrt{e}-1\right)}\sum_{i=1}^{n}\left[\mu_A\,(x_i)\,e^{1-\mu_A(x_i)} - \left(1-\mu_A\,(x_i)\,e^{1-\mu_A(x_i)}-1\right)\right] \quad (8)$$

where $n$ is the length of data set, $\mu_A$ is the membership function of fuzzy set $A$ and $x_i$ is the supporting points of the fuzzy set $A$ and min is the minimum value.

### *3.2.4 Morphology-based edge detection (Block C)*

Morphological edge detection algorithm selects appropriate structuring element of the processed image and makes use of the basic theory of morphology, including erosion, dilation, opening and closing operation, and the synthesization operations to get clear image edge. In the process, the synthesized modes of the operations and the feature of structuring element decide the result of the processed image. In detail, the synthesized mode of the operations reflects the relation between the processed image and original image, and the selection of structuring element decides the effect and precision and the result. Therefore, the keys of morphological operations can be generalized for the design of morphological filter structure and the selection of structuring element. In medical image edge detection, we must select appropriate structuring element by texture features of the image. The size, shape, and direction of structuring element must be considered roundly. Usually, except for special demand, we select structuring element by $3 \times 3$ square.

The basic operators of binary morphology are erosion, dilation, opening, and closing. In this paper, a mathematical morphology edge-detection algorithm is used. Opening-closing operation is first used as pre-processing to filter noise. Then the image is smoothened first by closing and then by dilation. The perfect image edge will be obtained by determining the difference between the processed image by above process and the image before dilation [24].

### *3.2.5 Border thinning*

Border detection algorithms detect borders whose width consists of more that one pixel. To reduce the borders' width to one pixel,pixels chains are built that characterize borders. We have used the Susan thinning algorithm [19]. In this algorithm, a pixel is measured and consider border pixel if at least one of its neighbors is white. In this way, a border chain is built that is a set of connected border pixels. The algorithm starts considering all the pixels as border chains. Then it eliminates the pixels for each chain in such a way that these eliminated pixels do not influence the border connectedness. In this way, it produce an image with one-pixel contours (see Fig. 7f).

### *3.2.6 Lung border recognition*

The two pulmonary lobes are selected after determining the thinned border chains. This selection mechanism is different for the different slices in the CT-scanned images. For this purpose, first the border chains less than a constant threshold (17 pixels in our experiments) are eliminated for all slices. Then the two longest border chains are selected as pulmonary lobes, and these largest border chains are chosen as lungs [14].

### *3.2.7 Lung border rebuilding*

During thresholding and border recognition, it is possible that some nodules adjacent to the pleura are identified as belonging to the chest and, therefore, suppressed. Therefore, it is compulsory to rebuild the pulmonary lobe border that has been wrongly eliminated. The method used for the border rebuilding is shown in Fig. 8.

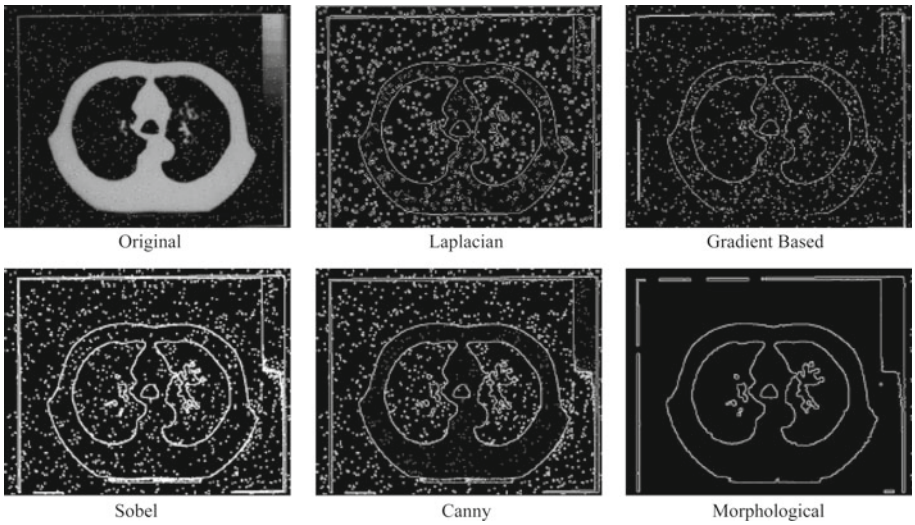


**Fig. 7** Results of edge detection block

**Lungs Border Rebuilding Algorithm**

**Input:** Image after Thinning Lungs border, threshold T
**Output:** Reconstruction of Lungs border
**Procedure**
*For each pair of border pixels*
*Step 1: Compute* $d_1$
$$d_1 = (x_2 - x_1)^2$$
*Step 2: Compute* $d_2$
$$d_2 = (y_2 - y_1)^2$$
*Step 3: Compute ratio r*
$$r = d_2/d_1$$
*Step 4:*
*if* $(r \geq T)$
*pixel is candidate for reconstruction*
*else*
*skip pixel*
*endif*
*endfor*
*Step 6: Exit*

**Fig. 8** Lung border rebuilding algorithm

### *3.2.8 Lung area filling*

After rebuilding the lung borders, it is necessary to identify the set of pixels belonging to the internal part of the two pulmonary lobes. Then these pixels have to restore their initial gray level. We have used a region filling technique. We have selected a pixel randomly inside the pulmonary lobes and mark it. We enlarge the region by visiting the neighboring pixels and marking them until we reach the border. To restore the gray levels is now easy and the results obtained are shown in Fig. 7i. Then we have superimposed these two thinned chains representing the lung lobes on the original lungs CT scan image to show the accuracy of

our method in identifying the pulmonary regions. For nodule detection, the region has been highly reduced. We have eliminated all the external structures except lungs lobes. Simple thresholding allows us to isolate the internal part of the lung, i.e., blood vessels, bronchi and nodules.

## 4 Data sets and characteristics

The FEMS system was implemented by using the MATLAB [9] environment. We obtained datasets from Aga Khan Medical University, Pakistan. The following are the major characteristics of the input images:

1. $256 \times 256$ pixels of each image
2. 8-bit grey scale images (255 grey levels)
3. Slice thicknesses of changing data
4. The lung cavities also have pathology in certain cases.

The collaboration with Aga Khan University Hospital for this research project made it possible to get the database from Aga Khan University Hospital Karachi. The CT-scanning facilities available at the hospital are the best available in Pakistan [8]. The embedded UNIX-based computing systems of the CT scan equipment are interfaced with windows machines as well which led to an easier exporting of the CT scan data. Complete cases for nine patients were acquired from AKU which were axial CT scan slices at a slice width of minimum of 5 mm. The most common standard for receiving scans from hospital is DICOM. While the analyze format is required for image-processing algorithms. Thus there is need of converting DICOM images to analyze format. A single DICOM file contains both a header (which stores information about the patient's name, the type of scan, image dimensions, etc.), as well as all of the image data (which can contain information in three dimensions). This is different from the popular Analyze format, which stores the image data in one file (*.img) and the header data in another file (*.hdr).The DICOM software provides Export utility that can export DICOM format file to different analyze formats. The DICOM software provides export utility that can export DICOM format file to different analyze formats like: JPEG, BMP, TIFF, PCX, PNG, WMF, TGA, EMF, etc. As JPEG format is lossy compression and in case of medical images a loss of single bit may cause misdiagnosis of the disease, we have selected TIF format which is lossless compression format. All images are converted into TIF for further processing.

## 5 Results and discussion

In this work, we have studied the performance of the different segmentation techniques that are used in Computer Aided Diagnosis (CAD) systems using thorax CT Scans. These methods for segmentation give good results on test databases of reasonable size. There is still much room to work on Computer Aided Diagnosis in CT scan imaging. CT lung density is influenced by the factors such as subject tissue volume, air volume, image acquisition protocol, physical material properties of lung parenchyma and trans-pulmonary pressure. These factors make the selection of gray-level segmentation threshold difficult, as different thresholds are likely required for different subjects. The selection of optimal threshold by iterative method is one possible solution. But again due to different density of anatomical structures on each slice as discussed above, there is need of computing the threshold for each

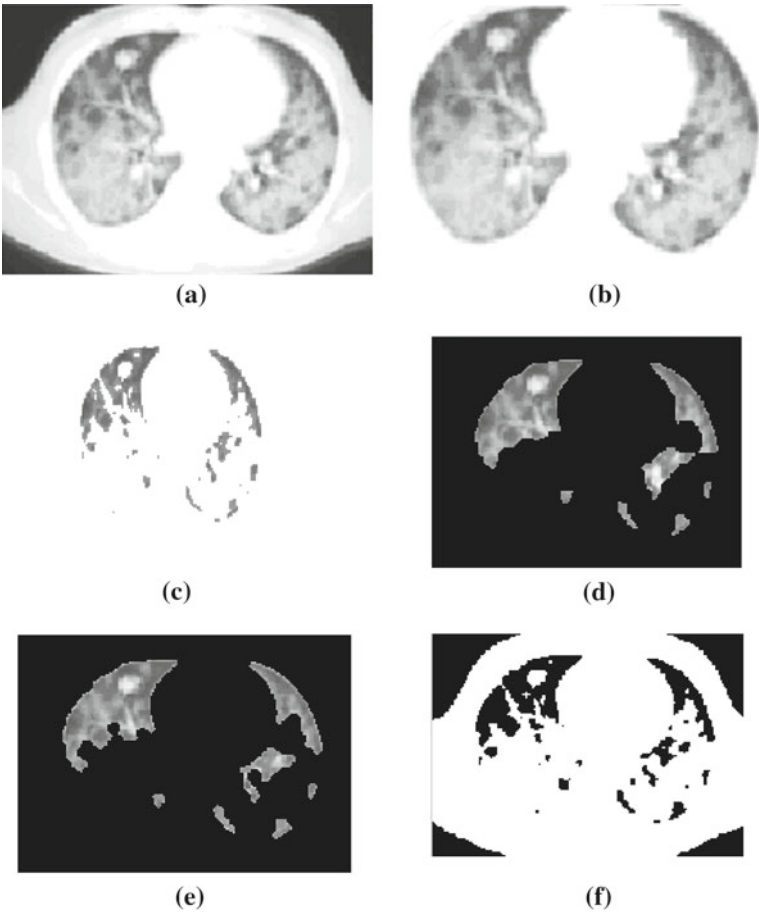


**Fig. 9** Comparison of results of different algorithms with our FEMS system. **a** Original image, **b** FEMS algorithm, **c** Antonelli et al. [14], **d** Hu [21], **e** Samuel et al. [20], **f** El-Baz [4]

slice which is costly from computational point of view. Thus, there is a need of sophisticated algorithm which can calculate a single threshold for entire database of a single patient. Also, the algorithms reported so far have used the databases of slice thickness usually varying in (5–10 mm). But, with the advent of modern MSCT scanners and their possibility to acquire sub millimeter slice data over the whole thorax with a single breath-hold, software algorithms for CAD for the diagnosis of lung cancer must be improved using these databases having slice thickness of 1 mm or less.

The segmentation algorithm starts off with the basic pre-processing of the image by either appending a one-pixel wide black boundary or setting the outermost boundary layer of the image to zero intensity. This is necessary to ensure that if the seed pixel selected once shall suffice to delete all the background regions by region-growing when the process starts. Thus, we ensure that for each region of background, we will not have to select a seed-pixel for region growth. The optimum threshold for a particular data set in CT depends on the following basic factors—tissue volume, air volume, density units of tissue, image acquisition methodology and properties of contrast in the image owing to the lung parenchyma

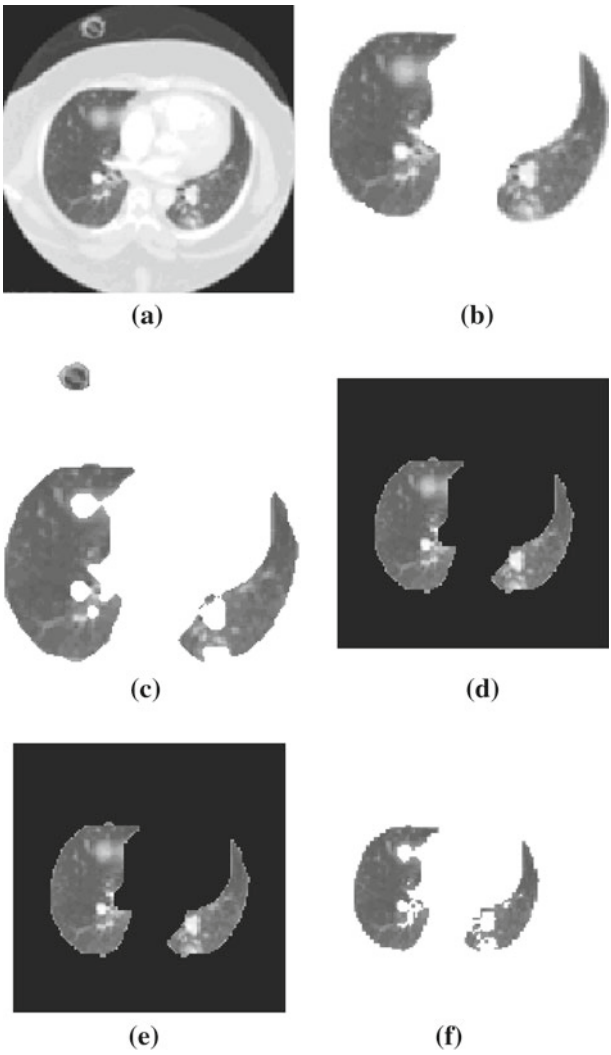


**Fig. 10** Comparison of results of different algorithms with our FEMS system. **a** Original image, **b** FEMS algorithm, **c** Antonelli et al. [14], **d** Hu [21], **e** Samuel et al. [20], **f** El-Baz [4]

(lung tissue). Since these factors may vary with each case and for each $512 \times 512$ image within a case, the optimum threshold is selected for each and every image in each and every case that is encountered. Generally, there is little variation in the threshold across repeated scans of the same subject while miniature differences exist when conducting the study across subjects. Optimum thresholding performs better when lung volumetric differences are unavoidable.

Figure 9b gives the result of our FEMS technique on the test image. It is evident through observation that the FEMS system produces much smoother results than the schemes that have been used earlier. It can be proved that nearly all previous techniques do not work for the images when there is overlapping of intensities in lung parenchyma and surrounding chest wall. However, out FEMS technique has shown promising results on the different test cases as shown in figure. Results of our FEMS method that are shown in Fig. 9b demonstrate

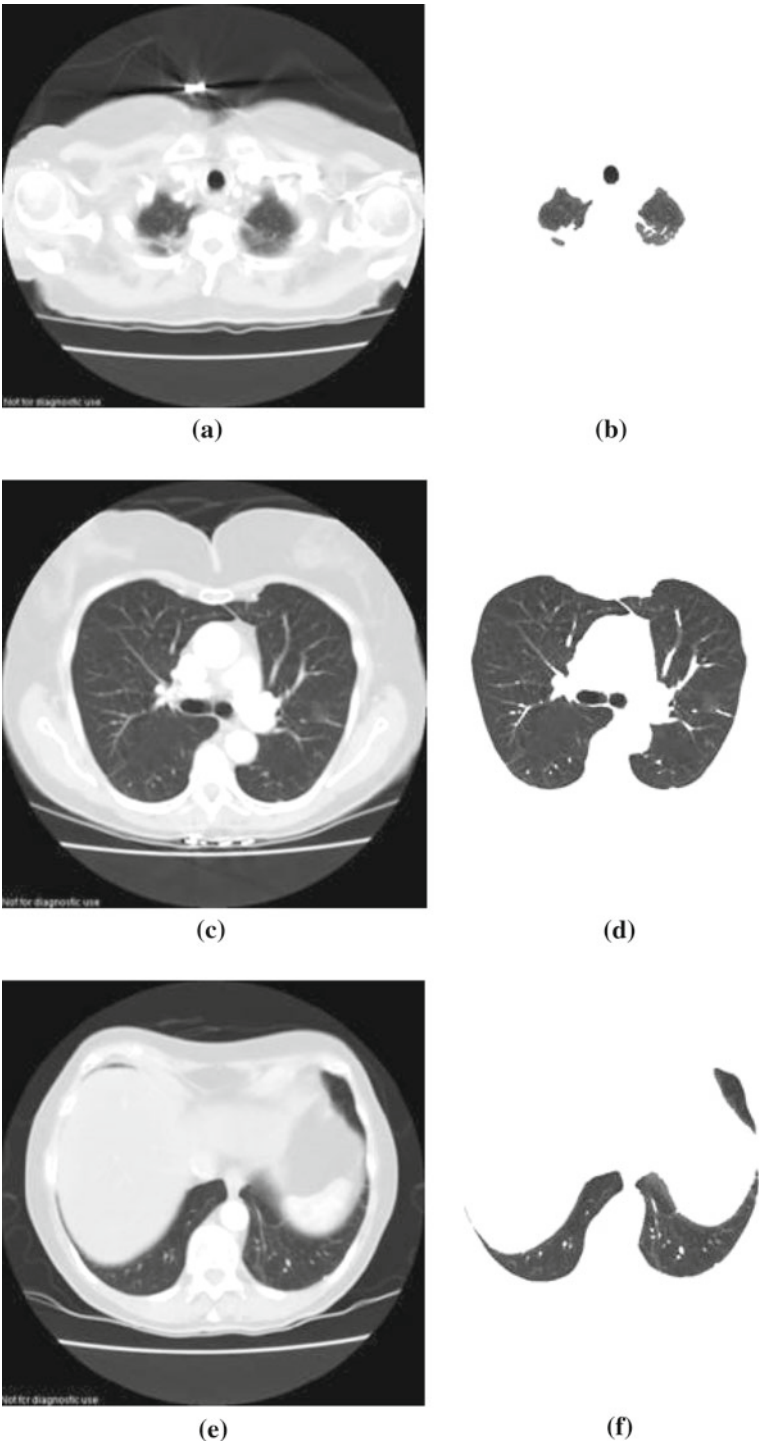


**Fig. 11** FEMS method results on different CT Scan images. **a** Original image, **b** FEMS algorithm, **c** Original image, **d** FEMS algorithm, **e** Original image, **f** FEMS algorithm, **g** Original image, **h** FEMS algorithm

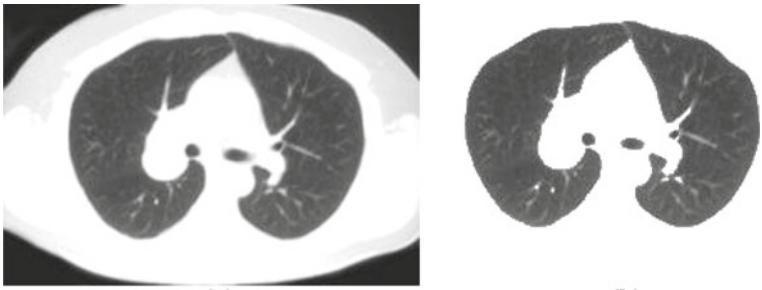


**Fig. 11** Continued

significant improvement. The figure shows that using our method, we are able to segment the image almost completely, thus, extracting lung part from the original image. There is also no loss of lung nodules in our FEMS method. This is a good advancement for next stage of CAD system employed in lungs nodule detection and classification system.

Figure 10b gives the result of our FEMS technique on the test image. It is evident through observation that the FEMS system produces much smoother results than the schemes that have been used earlier. It can be proved that nearly all previous techniques don't work for the images when there is overlapping of intensities in lung parenchyma and surrounding chest wall. However, out FEMS technique has shown promising results on the different test cases as shown in figure. Results of our FEMS method that are shown in Fig. 10b demonstrate significant improvement. The figure shows that using our method, we are able to segment the image almost completely, thus, extracting lung part from the original image. There is also no loss of lung nodules in our FEMS method. This is a good advancement for next stage of CAD system employed in lungs nodule detection and classification system. We have also tested our new FEMS method on different test images as shown in Fig. 11. Results of our FEMS method that are shown in Fig. 11b, d, f and h demonstrate significant improvement. The figure shows that using our method, we are able to segment the image almost completely thus extracting lung part from the original image.

The essence of our segmentation method lies in its ability to fully automatically segment the lungs part from whole CT scan image. Search for higher density structures including nodules scattered in the lungs through sequentially declining threshold level.

## 6 Conclusions and future work

We have described an adaptive and fully automatic method for segmentation of pulmonary parenchyma. The "heart" of the FEMS system, FCM that performs the adaptive thresholding, used to determine the thresholds and the error function based upon fuzzy entropy measures, was designed. This is just the first step of a CAD system which is still under development. The results we obtained are comparable with those of other known methods. In addition, the FEMS system has the advantage that it does not require any human expert intervention or any a priori information to the number of clusters (segments) that appear in the image.

The next steps we are working on are nodule detection and false positive reduction. In particular, as regards nodule detection, we are currently investigating both 2-D and 3-D algorithms to distinguish between nodules, bronchial structures, and blood vessels. The method of lung segmentation presented in this paper can provide any thoracic image containing varying textures.

Not only does it performs efficiently on normal images, but also works equally well on images containing abnormality patches and nodules at any part of the lung, as verified by the results in Figs. 7 and 5. Methodologies used in [3,14,20,21] show a serious shortcoming when they encounter abnormal thoracic CT images, containing abnormality at the margins, which is a common case in images of most of the fatal lung diseases, like Cancer, TB etc. Future focus is to develop a method that automatically detects nodules within the lung part and then to classify images.

**Acknowledgments** Two of the authors, Mr. M. Arfan Jaffar, 041-103525-Cu-031 and Mr. Ayyaz Hussain, 042-310554-Eg2-360 would like to acknowledge the Higher Education Commission of Pakistan for providing the funding and required resources to complete this work. It would have been impossible to complete this effort without their continuous support.

## References

1. Cilva AC, Cezar P, Gattas M (2004) Diagnosis of Lung Nodule using Gini Coefficient and skeletoniz in computerized Tomography images. In: ACM symposium on applied computing, Nicosia, Cyprus, pp 243–248
2. Dhawan AP (2003) Medical image analysis IEEE press series in biomedical engineering. Wiley, London
3. El-Baz A, Farag AA, Falk R, La Rocca R (2002) Detection, visualization and identification of lung abnormalities in chest spiral CT scan: Phase-I. In: International conference on biomedical engineering, Cairo, Egypt
4. El-Baz A, Farag AA, Falk R, La Rocca R (2003) A unified approach for detection, visualization and identification of lung abnormalities in chest spiral CT scan. In: Proceedings of computer assisted radiology and surgery, London
5. Zhao B, Gamsu G, Ginsberg MS (2003) Automatic detection of small lung nodules on CT utilizing a local density maximum algorithm. J Appl Clin Med Phys 4(3)
6. Cesario E, Folino F, Locane A, Manco G, Ortale R (2008) Boosting text segmentation via progressive classification. Knowl Inf Syst 15:285–320
7. Hoffman EA, McLennan G (1997) Assessment of the pulmonary structure-function relationship and clinical outcomes measures Quantitative volumetric CT of the lung. Acad Radiol 4(11):758–776
8. http://www.aku.edu/
9. http://www.mathworks.com
10. Bezdek JC (1981) Pattern recognition with fuzzy objective function algorithms. Plenum Press, New York
11. Dehmeshki J, Ye X, Valdivieso M (2007) Automated detection of lung nodules in CT images using shape-based genetic algorithm. Comput Med Imaging Graph 31(6):408–417
12. Chuang K, Tzeng H, Chen S, Wu J, Chen T (2006) Fuzzy c-means clustering with spatial information for image segmentation. Comput Med Imaging Graph 30(1):9–15
13. Rebelo MS, Furuie SS, Gutierrez MA, Costa ET, Moura LA (2007) Multiscale representation for automatic identification of structures in medical images. Comput Biol Med 37(8):1183–1193
14. Antonelli M, Lazzerini B, Marcelloni F (2005) Segmentation and reconstruction of the lung volume in CT images. In: 20th annual ACM symposium on applied computing, vol I. Santa Fe, New Mexico, pp 255–259, 13–17 March
15. Memon NA, Mirza AM, Gilani SAM (2006) Deficiencies of Lung segmentation techniques using CT scan images for CAD. In: Proceedings of world academy of science, engineering and technology, vol 14
16. Memon NA, Mirza AM, Gilani SAM (2006) Segmentation of lungs from CT scan imges for early diagnosis of lung cancer. In: Proceedings of world academy of science, engineering and technology, vol 14
17. Haiminen N, Gionis A, Laasonen K (2008) Algorithms for unimodal segmentation with applications to unimodality detection. Knowl Inf Syst 14:39–57
18. Gwadera R, Gionis A, Mannila H (2008) Optimal segmentation using tree models. Knowl Inf Syst 15:259–283
19. Smith SM, Brady JM SUSAN (1997) A new approach to low level image processing. Int J Comput Vis 23(1):45–78
20. Armato SG III, Giger ML, Moran CJ (1999) Computerized detection of pulmonary nodules on CT scans. RadioGraphics 19:1303–1311

21. Hu S, Huffman EA, Reinhardt JM (2001) Automatic Lung Segementation for Accurate Quantitiation of Volumetric X-Ray CT images. IEEE Trans Med Imaging 20(6)
22. Boskovitz V, Guterman H (2002) An adaptive neuro fuzzy system for automatic image segmentation and edge detection. IEEE Trans Fuzzy Syst 10(2):247–262
23. Xie XL, Beni GA (1991) Validity measure for fuzzy clustering. IEEE Trans Pattern Anal Mach Intell 3:841–846
24. Yu-qian Z, Wei-hua G, Zhen-cheng1 C, Jing-tian1 T, Ling-yun L (1997) Medical Images Edge Detection Based on Mathematical Morphology. In: Proceedings of the IEEE engineering in medicine and biology 27th annual conference Shanghai, China

## Author Biographies

**M. Arfan Jaffar** received his B.Sc degree from Bahauddin Zakariya University Multan, Pakistan in 2000 and got distinction (Gold Medal). He later received M.Sc. degree in computer science in 2003 from Quaid-e-Azam University Islamabad, Pakistan. Then he earned his M.S. degree in computer science in 2007 from National University of Computer and Emerging Sciences, NU-FAST, Islamabad, Pakistan. Currently he is pursuing his Ph.D. research at the Department of Computer Science, NU-FAST. His research interests include image processing and computational intelligence.

**Ayyaz Hussain** received his M.Sc. degree in computer science in 2000 from Quaid-e-Azam University Islamabad, Pakistan, and his M.S. degree in computer science in 2007 from National University of Computer and Emerging Sciences, NU-FAST, Islamabad, Pakistan, and got distinction (Bronze Medal). Currently he is pursuing his Ph.D. research at the Department of Computer Science, NU-FAST. His research interests include image processing and computational intelligence.

**Dr. Anwar Majid Mirza** is professor at the National University of Computer and Emerging Sciences (FAST-NUCES), Islamabad, Pakistan. He is keenly interested in the areas of design and analysis of Neuro-Fuzzy Systems, Image Processing, Artificial Intelligence and Computational Physics. He has successfully supervised four PhD students towards the doctorate at GIKI. He is currently supervising eight Higher Education Commission sponsored PhD scholars working in the areas of Evolutionary Programming, Pattern Recognition, Image Restoration, Medical Imaging and Wavelet- and Finite Element- solution of partial differential equations. His PhD research work on modeling and simulation has been cited at numerous places including the book entitled “Finite Element Methods for Particle Transport” published by John Wiley & Sons in 1997.